

# The Large Magellanic Cloud cluster NGC 2214

Timothy Banks,<sup>1</sup> R.J. Dodd<sup>2</sup> and D.J. Sullivan<sup>1</sup>

<sup>1</sup>*Department of Physics, Victoria University of Wellington, PO Box 600, Wellington, New Zealand*

<sup>2</sup>*Carter Observatory, PO Box 2909, Wellington, New Zealand*

Accepted 1995 January 29. Received 1995 January 17; in original form 1994 September 12

## ABSTRACT

Johnson *BV* CCD observations have been made of the young Large Magellanic Cloud cluster NGC 2214 and a nearby field using the Anglo-Australian Telescope. It has been suggested in the literature that this elliptical cluster is actually two clusters in the process of merging. No evidence is found from profile fitting or the colour–magnitude diagrams to support this contention. Completeness factors are estimated for the CCD frames. These values are used in conjunction with luminosity functions to estimate the initial mass function (IMF) for NGC 2214. A power law is assumed for the IMF, with a good fit being found for the exponent  $(1 + x) = 2.01 \pm 0.09$ . There is some indication that the low-mass end ( $\approx 3 M_{\odot}$ ) has a lower gradient than the high-mass end of the derived IMF. This value is in reasonable agreement with literature values for other Magellanic IMFs, and not substantially different from those of the poorly determined Galactic IMFs, suggesting the possibility of a ‘universal’ IMF over the Magellanic Clouds and our Galaxy in the mass range  $\sim 1$  to  $\sim 10 M_{\odot}$ .

**Key words:** Star Clusters – Large Magellanic Cloud

## 1 INTRODUCTION

NGC 2214 ( $\alpha_{2000} = 6^{\text{h}} 12^{\text{m}} 57^{\text{s}}$ ,  $\delta_{2000} = 68^{\circ} 15' 33''$  South) is a young ( $32 \times 10^6$  yr; Elson 1991) populous star cluster situated in a relatively uncrowded field to the far north-east of the bar in the Large Magellanic Cloud (LMC). Meylan & Djorgovski (1987) analysed an intensity profile of the cluster, and found that the core was abnormal. They conjectured that perhaps it had collapsed, although Elson, Fall & Freeman (1987) have shown that the two-body relaxation time of the cluster is  $\sim 2 - 6 \times 10^8$  yr, and so greater than its age. Bhatia & MacGillivray (1988) found the cluster to have a very elliptical ( $e = 0.5$ ) core with an almost spherical halo, and suggested that this unusual shape could be due to NGC 2214 being a binary star cluster in an advanced stage of merging. Comparison with N-body simulations lent support to this idea. Sagar, Richtler & de Boer (1991a) used the 1.54-m ESO Danish telescope in  $\sim 1$ -arcsec seeing, and presented a *BV* colour–magnitude diagram (CMD) with two well-defined supergiant branches, separated by  $\sim 2$  mag in *V*. The older population was more centrally condensed than the younger one, and Sagar et al. (1991a) suggested that the first published CMD (Robertson 1974) had failed to detect the older branch due to the problems of photometry in such a crowded region.

A major objective of the present study was to derive an estimate of the initial mass function (IMF) of the cluster. The IMF is defined as the frequency distribution of stellar masses on the main sequence at the formation time of a

group of stars (Scalo 1986). Mass is one of the primary factors influencing stellar evolution, and a detailed knowledge of the IMF would be important in a wide range of studies ranging from galactic evolution to the spectral properties of binary stars (see Tinsley 1980). A fundamental question about the IMF is whether it is universal in time and location, or whether the distribution of stars formed is a function of parameters such as metallicity.

Derivation of the IMF is not straightforward. An initial approach might be to use the nearby solar neighbourhood to do this, but this technique is complicated by the fact that these stars have a range of distances, ages, and metallicities. For instance, the random velocities of the stars, combined with their lifetimes, means that, while massive stars will still be near the site of their formation, low-mass stars will have travelled significant distances. Variations in composition may result just from such spatial considerations, if not from galactic evolution as well. Scalo (1986) comments that the many assumptions, such as any variation in the star formation rate with time, complicate estimates of the field IMF to the point of impracticality. In addition, a universal nature is assumed for the IMF in such studies.

A better approach is to use clusters, where the component stars will be effectively coeval and of the same composition. Such work is complicated by effects such as dynamical evolution leading to mass segregation in the cluster, tidal stripping (which in the presence of mass segregation will lead to the proportional decrease of low-mass stars; see Spitzer

1987), and stellar evolution as stars evolve off the main sequence, which leads to no easily derivable mass function information for stars of a main sequence lifetime less than the age of the cluster. The mass function of the cluster may alter substantially with time, and it is best to select young clusters where these effects have not had time to become significant. Many studies have centred on young Galactic open clusters with their large observable mass range (e.g. Phelps & Janes 1993; Reid 1992; Stauffer et al. 1991). However, such work is complicated by field star contamination, counting incompleteness, and low number statistics (see Scalo 1986 for more details), as well as the problem that most open clusters suffer substantial and variable reddenings due to their positions in the Galactic disc (Mateo 1988). There is no strong evidence for variations in the shapes of their mass functions (Sagar & Richtler 1991). Globular clusters offer better statistics due to the increased number of stars they contain, but the observable mass range is limited due to their distances and age. Evolutionary effects, such as mentioned above, are additional complications. The resulting mass functions appear to vary considerably between clusters, and may be correlated with metallicity (Sagar & Richtler 1991), although this is clouded by the above problems.

The LMC clusters are effectively a mixture of the best features of these two types of star clusters. They are populous, with resultingly good statistics, and span a wide range of ages and metallicities (Da Costa 1991). The clusters are distant enough to subtend only a small angle on the sky, and yet not too distant to suffer from resolution problems. Questions, such as the universal nature of the IMF, might be able to be addressed using these clusters, although the very populous nature of both the clusters and their fields leads to counting incompleteness problems. A major portion of this study involved the derivation of counting estimates, in order to correct observed luminosity functions to the ‘real’ distribution.

IMFs have been derived for some LMC clusters by Mateo (1988), Sagar & Richtler (1991), Cayrel, Tarrab & Richtler (1988), and Elson, Fall & Freeman (1989). The results have not been in good agreement. The first three studies were based on CCD frames, and attempted to estimate the counting incompleteness using artificial star trials (see below). A power law  $\frac{dN}{dM} = M^{-(1+x)}$  was assumed for the IMF, where  $dN$  is the number of stars in a given mass interval  $dM$  at mass  $M$ . Mateo (1988) found that the IMFs of six Magellanic clusters (the Small Magellanic Cloud cluster NGC 330 was included) could all be fitted with the single power law with  $x = 2.52 \pm 0.16$  over the mass interval 0.9 to  $10.5 M_{\odot}$ . Sagar & Richtler (1991) used a different method of estimating the incompleteness (see below), and arrived at an  $x$  value of  $\sim 1.1$ , not too different from the Salpeter (1955) value of 1.35 and in reasonable agreement with the value of 1.2 for NGC 330 and NGC 1818 derived by Cayrel et al. (1988). They commented that if they used the same incompleteness technique as Mateo (1988) on NGC 1711, which was the only cluster studied by both, then the mass function estimate of Mateo (1988) was confirmed. All these values contrast sharply with the photographic star count analysis of Elson et al. (1989), which gave  $x$  values between  $-0.2$  and  $0.8$  (over  $1.5$ – $6.0 M_{\odot}$ ). In light of these differences and the comment of Sagar & Richtler (1991) about NGC 1711, a

review of the incompleteness techniques is obviously of major importance given the effect a chosen method has on the derivation of the mass function slope, and any subsequent conclusions about the universality of the IMF.

## 2 OBSERVATIONS

Johnson  $BV$  observations of NGC 2214 were collected on the night of 1993 March 1/2 using a 1024 by 1050 pixel TEK CCD at the prime focus of the Anglo-Australian Telescope. The pixel scale was 0.39 arcsec per pixel, resulting a field of view approximately  $6.7 \times 6.7$  arcmin square. The FWHM seeing was  $\sim 2.2$ -arcsec. Observations were also made of a field 5-arcmin north of the cluster. Exposure times for both these regions were 30 and 300 s in  $V$ , and 60 and 600 s in  $B$ .

The initial reductions of the CCD frames were carried out at the Anglo-Australian Observatory, and included trimming the frames of the overscan rows, subtraction of the mean of the overscan (the CCD has negligible bias structure), and flat-field division using sky flats. Given already derived extinction coefficients (Da Costa, private communication), the observed Graham (1982) E2 and E3 standards were used in the IRAF PHOTCAL package to derive the zero-point shift in the following transformation equations:

$$b = (1.067 \pm 0.007) + 0.12(B - V) - (0.4 - 0.02(B - V))X + B$$

$$v = (1.093 \pm 0.006) - 0.27X + V$$

where  $X$  is the airmass and the lower case letters refer to the observed instrumental magnitudes. The root mean squares of the fits were 0.018 and 0.016 mag for  $B$  and  $V$  respectively.

## 3 RESULTS

### 3.1 Colour–magnitude diagrams

The DIGIPHOT package of IRAF, which includes DAOPHOT (Stetson 1987), was used to reduce the crowded frames, perform aperture corrections, and transform the data across to the standard system. The final colour–magnitude diagrams are given as Figs 1 and 2. 2919 and 1832 stars are plotted in the cluster and field diagrams respectively. The matching point between the long and short exposures was chosen to be the region where the data sets had similar errors, and was magnitudes 16 and 17 for  $V$  and  $B$  respectively.

$\chi$  is the ratio of the actual scatter, about a point spread function (PSF) fit, divided by the expected scatter given the star and background sky brightnesses combined with the CCD readout noise. A value of  $\chi$  near unity indicates a good fit. Only stars with a  $\chi$  value of 3.0 or less were accepted (as in Mateo & Hodge 1986). Examination of  $\chi$  plotted against observational magnitude showed this to be an acceptable limit, with the vast majority of detected ‘stars’ being within it. A further constraint was the use of the ‘sharpness’ measure of the difference between the square of the width of the object and the square of the width of the PSF. Values should be close to zero for single stars, large and positive for blended doubles and partially resolved galaxies, and large and negative for cosmic rays and blemishes. Examination of this parameter for all detected ‘stars’ showed that the majority had values inside  $|0.2|$ . The final selection criterion was

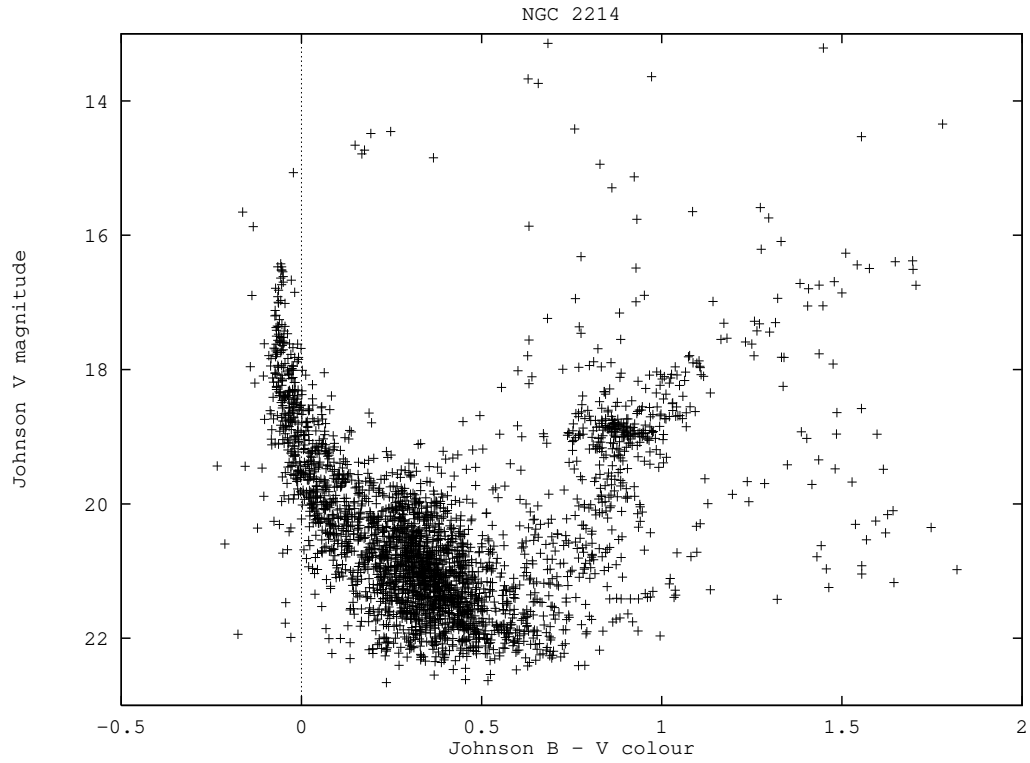


Figure 1. Colour-magnitude diagram for NGC 2214.

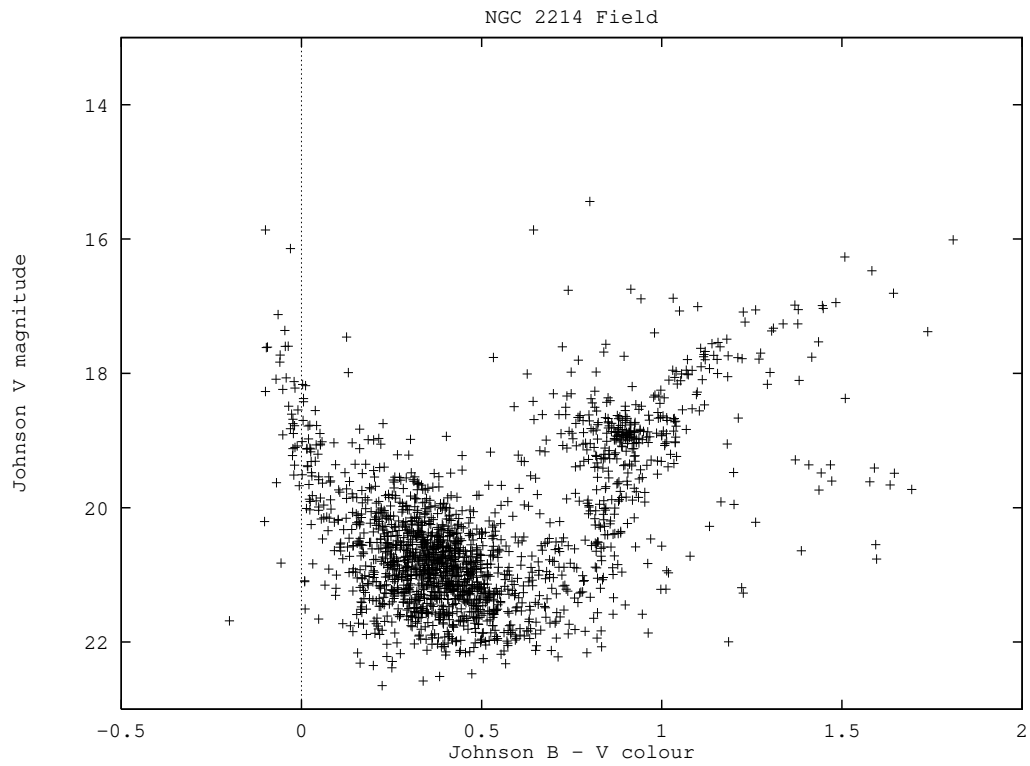
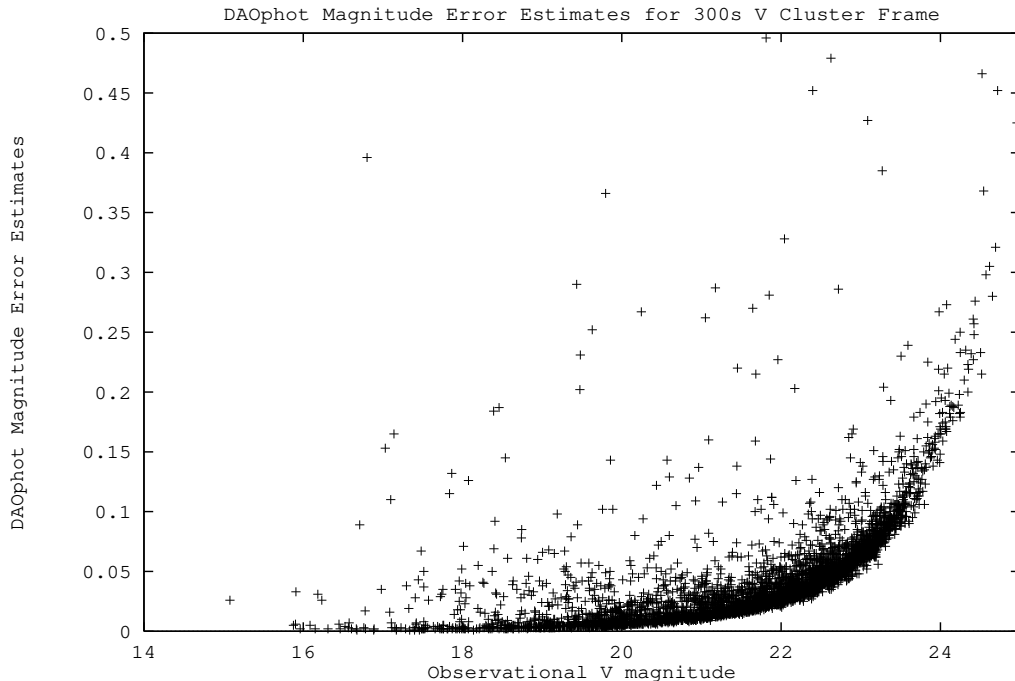


Figure 2. Colour-magnitude diagram for the Field.



**Figure 3.** Photometric Errors for the 300 second  $V$  exposure of NGC 2214.

**Table 1.** Adopted error limits. The majority of the photometric errors derived by DAOphot fall on to an exponential function. The error adopted for each observational magnitude range (as given in the table) corresponds to the value of this function at the fainter magnitude limit of each interval. The number of stars recovered in each bin is also indicated, under the headings ‘Cluster’ and ‘Field’ for each filter.

Johnson $V$				Johnson $B$			
Mag	Limit	Cluster	Field	Mag	Limit	Cluster	Field
10-16	0.010	16	1	10-17	0.001	22	2
16-18	0.011	56	13	17-18	0.005	33	5
18-19	0.016	111	54	18-19	0.013	109	22
19-20	0.025	349	139	19-20	0.018	236	103
20-21	0.040	504	291	20-21	0.028	550	317
21-22	0.060	925	644	21-22	0.040	886	578
22-23	0.090	1045	811	22-23	0.063	1055	873
23-24	0.200	287	207	23-24	0.120	568	349
Total:	-	3293	2160	Total:	-	3459	2249

the use of photometric error estimates from DAOphot. Photometric errors, as determined from least-squares fitting by DAOphot, naturally increase with magnitude (see Figs 3). If a low threshold were set for the acceptable errors across all the data, the fainter magnitudes would be excluded. In order to retain as many as possible of these fainter stars in the CMD, the acceptable photometric uncertainty was relaxed as magnitude increased. These values are given in Table 1.

The main features of the cluster CMD are the following.

- (i) A conspicuous main sequence of  $(B-V) \sim 0$  extending to  $V \sim 16.5$ .
- (ii) Evolved stars above this main sequence turnoff.
- (iii) A subgiant branch of  $(B-V) \sim 0.85$ , extending from  $V \sim 19$  to  $\sim 21$ .

(iv) A giant star clump at  $(V, B-V) \sim (19, 0.9)$  which is slightly extended in  $(B-V)$  by some 0.25. This extension is above the accepted photometric error at this  $V$  magnitude (see Table 1).

(v) A uniformly populated giant branch extending from the giant clump up to  $(V, B-V) \sim (16.5, 1.7)$ .

(vi) Several stars blueward of the main sequence, which are artefacts of the crowded field reduction (Lee 1992), being stars in dense regions whose parameters could not be estimated accurately by DAOphot. Magnitudes tend to be under-estimated. This is the basis of the bin migration phenomena noted by Mateo (1988), amongst others.

(vii) A clump peaking at  $(V, B-V) \sim (19.7, 0.3)$  of older stars.

(viii) Many faint red stars in the lower right of the CMD, which have been tentatively identified as giant stars by Chiosi (1989), and considered to be field stars.

Only items (i) and (ii) are features associated with the cluster, the others being due to field stars. Being at a moderate Galactic latitude ( $\sim -30^\circ$ ) the majority of field stars will be in the LMC. The field CMD appears to be contaminated to an extent by cluster stars, as evidenced by the reasonably strong main sequence.

As mentioned in the Introduction, Sagar et al. (1991a) presented a CMD for NGC 2214 with two supergiant branches, and claimed that, since the population of the older branch was more centrally concentrated than that of the younger one, previous studies would have missed them due to the increased level of crowding. The shallow  $BV$  CMD of Elson (1991) showed no sign of the second turnoff, although the  $\sim 5.5$ -arcsec seeing may have obscured it, as could the 3-arcsec seeing in the  $BV$  CMD of Banks (1993). However, examination of colour-magnitude diagrams for other LMC

clusters presented in Sagar, Richtler & de Boer (1991b) showed traces of second (weak) supergiant branches in other clusters. This, combined with the high number of stars blueward of the cluster main sequence, which are an indicator of crowded field reduction problems (Lee 1992), suggested that there may be problems with the reduction process. Short-exposure observations taken with the Mount John University Observatory (NZ) 1-m telescope gave some indication of a clump in the main sequence at the *V* magnitude corresponding to the older turnoff (Banks 1993; Banks, Dodd & Sullivan 1994). After submission of the observing proposal for the current study, which involved an investigation of the reality of the second branch, Lee (1992) published a paper describing CCD observations of NGC 2214 in 1.1-arcsec to 1.6-arcsec seeing with the Las Campanas du Pont 2.5-m telescope. The resulting *BV* CMD showed only one supergiant branch. The main sequence was matched well by a Maeder & Meynet (1991) isochrone for 50-Myr, while the supergiant branch was approximately matched by an older 70-Myr isochrone. The current study provides no evidence for a second supergiant branch.

CMDs were also generated for subsections of the frame, in order to search for differences across the cluster which might be expected for two merging clusters as in Bhatia & MacGillivray (1988). First the frame was split vertically about the cluster centre, which was estimated as the mean value derived from the ellipse fitting described below. The rotation of the cluster was also estimated as the mean value. Marginal distributions peak close by. Given that the position angle was  $\sim 100^\circ$ , this division effectively split NGC 2214 into the suggested merging halves. No difference was found in the shapes of the two CMDs, nor those for four  $300 \times 300$  pixel regions placed at  $90^\circ$  increments about the cluster centre, suggesting that if the merger idea is correct then the two bodies are of similar age (see also Bhatia & Piotto 1993, who came to the same conclusion).

### 3.2 Contours

Bhatia & MacGillivray (1988) presented contours of NGC 2214 based on a IIIaF UK Schmidt survey plate, which exhibited two lobes in the core of the cluster (see also Figs 4 and 5). Noting the possible criticism that isophotal maps may be influenced by the placement of bright stars, Bhatia & MacGillivray (1988) processed the COSMOS (MacGillivray & Stobie 1984) scans of the plates using a crowded field package in order to obtain star counts. They claimed these would not be strongly influenced by bright stars and so reflect more appropriately the distribution of stars in the cluster. Again a double peak was evident, although it can be seen that the contour delineating the peaks is not statistically different from the next 'lower' contour, which does not show lobes, if a Poisson distribution is assumed. It should also be noted that the IIIaJ plate contours presented by Bhatia & MacGillivray (1988) do not show a double peak, but rather show a slightly offset centre. This suggests that the lobes are due to a small number of stars, with markedly different colour indices.

The results of contouring the 30-s *V* frame of NGC 2214 are shown in Figure 4. As in Bhatia & MacGillivray (1988), two components appear to be in the cluster centre. Following Bhatia & MacGillivray (1988), stars were counted into

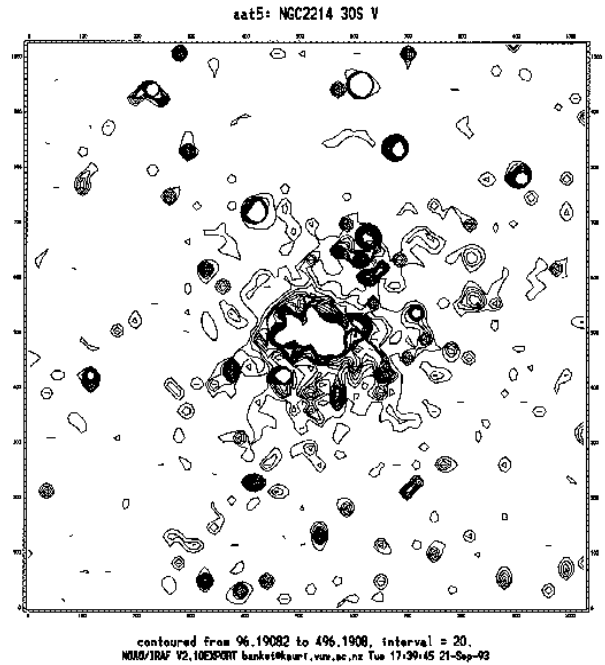


Figure 4. Contours for the outer regions of the 30-s exposure *V* frame of NGC 2214. The contour lines are increments of 20 counts per pixel over the range 96 to 496. Contours for the inner regions are shown in Figure 5.

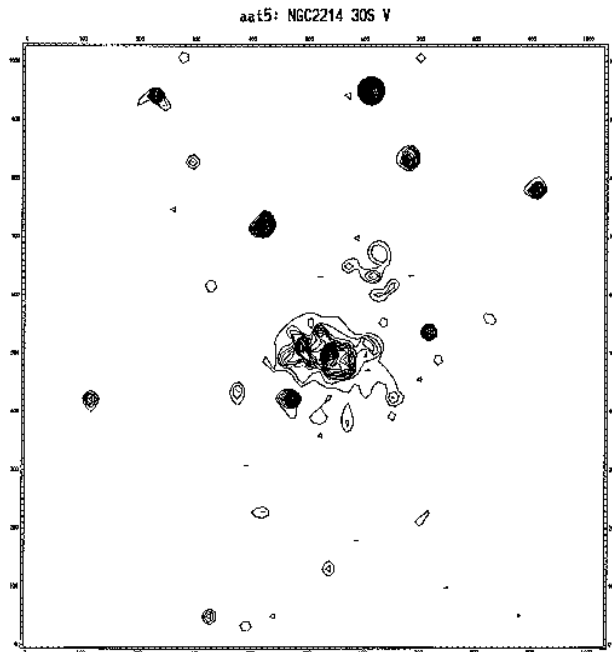
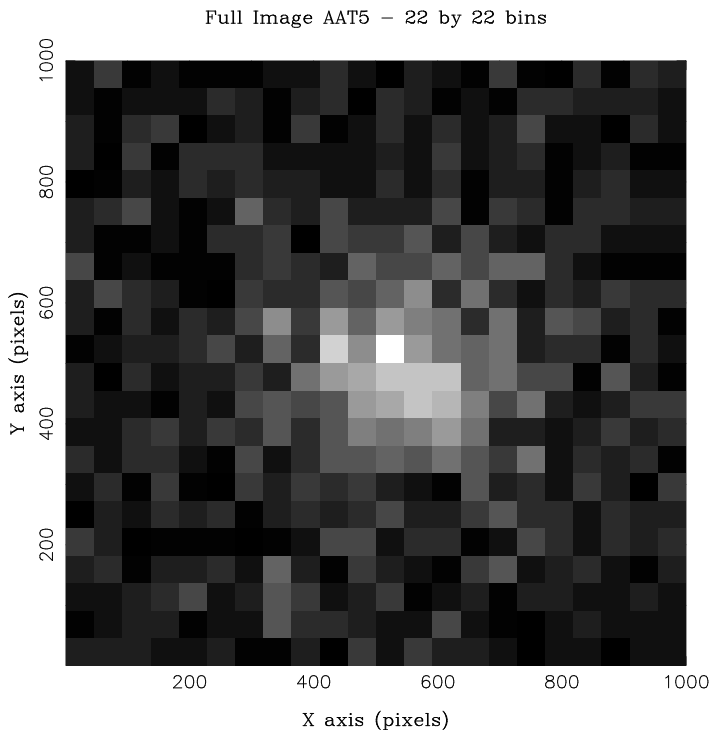
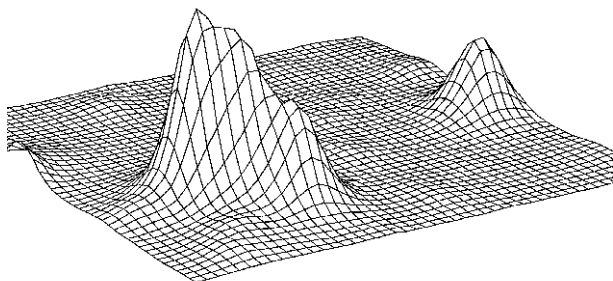


Figure 5. Contours for the inner regions of NGC 2214, in which contour levels range from 196 to 3196, with an increment of 100. Note the apparent double nature of the core, which should be compared with Fig. 2b of Bhatia & MacGillivray (1988).



**Figure 6.** 30-s *V* cluster frame star counts in 19.5-arcsec bins. White corresponds to the greatest number of stars (220 or more per square arcminute), while black corresponds to 15 or less stars per square arcminute.



**Figure 7.** Grid diagram of the blended region. A surface diagram, or a three-dimensional representation of a portion of the frame with intensity as the *z* (vertical) axis, shows that the gap between the two ‘cores’ contains the blended product of several bright stars. Each grid square represents one pixel.

$0.3 \times 0.3$  arcmin<sup>2</sup> bins, and each scaled to the number of stars per arcminute. A central condensation is evident, with a slight indication of a lobe, although a grey-scale representation of the data shows that the contour diagram tends to over-interpret the data (see Fig. 6). The central peak bin contained 20 stars, while the alleged secondary peak and gap between the two peaks contained 15 and 11 stars respectively. Assuming a Poissonian distribution, these latter two values are not statistically different.

Different selection effects apply to each of the bins, and so like is not being compared with like. The gap contains three of the four brightest stars in the bins. These stars, and the blended product shown in Fig. 7, could be obscur-

ing fainter stars. This would explain why the faintest star recovered in this bin is 2.5 mag brighter than that recovered in the less crowded ‘second lobe’. Certainly only the two outer stars were detected in the blended peak, with another further possible star being lost in the outer regions of the brightest star. The latter ‘star’ appears as a small rise in the outer regions of the point spread function (PSF) of the bright star when it is compared with the generic PSF derived for the frame.

The second peak is mainly outside the populated central region of the cluster, where blending is less severe. Fainter stars can be resolved, and so the star count increased. Star counts in populous clusters cannot naively be considered to reflect the underlying stellar distribution, due to problems deconvolving extremely crowded regions. A worst case scenario for a populous spherical cluster could show only a few star counts in the heavily blended inner regions, surrounded by a ring of greatest counts. From the centre of such a cluster, star counts would increase with radius until the radius of this ring was reached. Beyond this radius, the counts would drop away again.

An increase in the number of bins along each axis of the frame resulted in grey-scale plots of greater resolution, but with the tradeoff of less counts and greater noise. None of these plots showed any substantial evidence of a second component to the core. We contend that there is no evidence from star counts to support the notion that two cores are present in this cluster.

### 3.3 Ellipse fitting

Moment-based ellipse fitting was performed on the 60-s *B* frame of NGC 2214 using the routines described in Banks, Dodd & Sullivan (1995). A generally constant ellipticity of 0.4 was found out to a radius of  $\sim 30$ -arcsec from the cluster centre (see Fig. 8), before falling away to an ellipticity of 0.2 by  $\sim 40$ -arcsec. Beyond this radius the ellipticity is constant (out to the maximum measurement of 62-arcsec). The position angle was constant at  $\sim 100^\circ$  out to a radius of  $\sim 40$ -arcsec, and then climbed to another plateau at  $\sim 150^\circ$ . This may have been caused by the lower detection thresholds, used for the greater radii, encountering a grouping of a few stars to the side of the main body of the cluster, and so skewing the ellipse fit. These results agree well with the ellipse fitting of *V* CCD observations of NGC 2214 acquired at the Mount John University Observatory (NZ), which found similar trends and values even when the brightest stars were subtracted from the frame.

Zepka & Dottori (1987) fitted ellipses to photographic observations of NGC 2214, and found that the cluster ellipticity was constant at around 0.4 out to their maximum radius of 43-arcsec, and that the position angle of the clusters was constant. Frenk & Fall (1982) gave an ellipticity of 0.29 for their eye measurements of the burnt-out centre of NGC 2214 in an SRC Sky Survey plate. This result is in accord with those of the current study, as the measurement would correspond to outer regions of the cluster.

However, these apparent trends should be treated with caution, given the results of Banks et al. (1995) in which synthetic frames were generated of clusters with known ellipticities. Spurious trends were found by both the moment analysis technique used here, and the method of Jedrzejew-

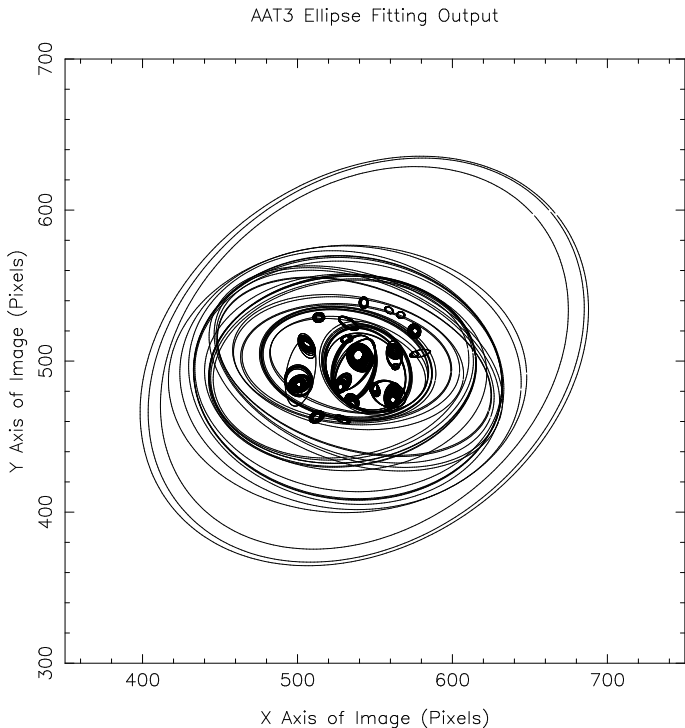


**Figure 8.** Ellipse fits to the 60-s  $B$  frame. The ‘lowest’ threshold used to detect pixels for ellipse fitting was 3 times the standard deviation of the background (which was in turn found by using the IRAF IMEX task in 21 regions across the frame).

**Table 2.** Isochrone fit ages. Logarithm of the ages are given for the best isochrone fits to these features in the CMDs. Different metallicities ( $Z$ ) were trialed. A distance modulus of 18.4 mag was assumed. The long and short moduli of 18.2 and 18.7 mag were also fitted, with no difference in ages for the modulus 18.2, while modulus 18.7 ages were log 0.2 younger. In the paper we have used the intermediate distance modulus of 18.4. The Swiss models are those of Schaerer et al. (1993), Schaller et al. (1992), and Meynet et al. (1993).

CMD Feature	Swiss models $Z =$			Bertelli et al $Z =$	
	0.001	0.008	0.020	0.004	0.020
Main Sequence:	-	8.0	8.0	8.3	8.2
Supergiant Branch:	-	7.8	7.8	8.0	7.9
Red Giant Clump:	8.7	8.7	8.6	-	9.0

ski (1987) as implemented in STSDAS, due to bright stars, some of which were so badly blended in crowded regions that they could be neither detected nor cleanly subtracted.

The ellipse fitting provides no definitive support for a double core to the cluster.

### 3.4 Isochrone fits

Initially both non-overshooting and overshooting isochrones were constructed with metallicity  $Z = 0.001$ , 0.008, and 0.020 (Schaerer et al. 1993; Schaller et al. 1992; Meynet, Mermilliod & Maeder 1993). Fits to features in both the cluster and field CMDs were attempted (see Table 2). The data points were transformed for a distance modulus of 18.4

and reddening of 0.08 (see Lee 1992; Castella, Barbero & Geyer 1987; Elson 1991). The  $V$  extinction was taken to be 3.1 times  $E(B - V)$  (Rieke & Lebofsky 1985; Mateo 1988; Sagar & Richtler 1991).

The 0.001 isochrones did not fit the features of the CMD at all well, being too blue. The fit to the red giant clump was poor, due to different gradients. Similarly the gradient of the giant branch was too steep. Non-overshooting models, at all three metallicities, did not fit this feature well either. However, the overshooting  $Z = 0.020$  isochrones did fit the branch well, but not the field giant clump and the main sequence at the fainter magnitudes.

$Z = 0.020$  isochrones fitted all features of the CMD best, with the  $Z = 0.008$  isochrones slightly too blue. The ages in Table 2 tend to depend more on the  $V$  magnitude axis than on colour, explaining the similarity of ages derived using the different metallicities. It was not possible with any of the isochrones to have one fit simultaneously the main sequence and the supergiant branch of the cluster. Lee (1992) used the Maeder & Meynet (1991) isochrones, and encountered the same problem, having to assign different logarithm ages of 7.7 and 7.8 respectively to these features. Sagar et al. (1991a) gave a range of ages for their ‘bright’ supergiant branch, ranging from the log value 7.5 using the Castellan, Chieffi & Staniero (1990) isochrones, to the log value 8.0 using Bertelli et al. (1990). The lower age was also derived by Elson (1991), based on the models of Becker (1981) and Brunish & Truran (1982). Our results tend towards the upper end of this age range, since we have used models incorporating convective overshooting, being, as are the other age estimates, dependent on the model used to derive the isochrones.

Turning to another set of models, the  $Z = 0.020$  isochrones of Bertelli et al. (1990) fitted the majority of the CMD features well (see Fig. 9), confirming the comment of Sagar et al. (1991a) that this metallicity is the best fit from the Bertelli et al. (1990) tables of  $Z = 0.020$ , 0.004, and 0.001.\* Again (see Table 2) two isochrones were needed to fit the upper main sequence and the supergiant branch well, although a shift of  $\sim +0.035$  in  $(B - V)$  would allow the 100-Myr isochrone to fit both. Such a shift is just outside the formal errors in the combined aperture corrections and photometric transformations. The same shift would allow the  $Z = 0.020 \times 10^7$  yr isochrone of Schaller et al. (1992) to fit both features well. However, fits to the upper main sequence lower metallicity isochrones can also be made with appropriate extra reddenings, although the fit to fainter features in the CMD worsens. NGC 2214 lies in a region of  $\sim 5 \times 10^{19}$  H I atoms per  $\text{cm}^2$  (a column density), according to the Mathewson & Ford (1983) map of the Magellanic Stream.

\* This is interesting in light of the Richtler & Nelles (1983) Strömgren estimate of  $[\text{Fe}/\text{H}] = -1.2 \pm 0.2$ , which would make NGC 2214 the least metal-abundant of all the young LMC clusters (see Da Costa 1991). Richtler & Nelles (1983) also give  $[\text{Fe}/\text{H}]$  values of  $-1.6$  and  $-1.8 \pm 0.2$  for the Magellanic Cloud clusters NGC 1818 and 330 (the latter being in the SMC). Later values for these clusters are  $-0.9$  (Richtler, Spite & Spite 1989) and  $-1.3$  (Spite et al. 1986), both using high-dispersion spectra, suggesting that Richtler & Nelles’ (1983) estimate for NGC 2214 is too metal-poor. See also Jasniewicz & Thévenin (1994) who found values of  $-0.37 \pm 0.03$  and  $-0.55 \pm 0.04$  for the two clusters.

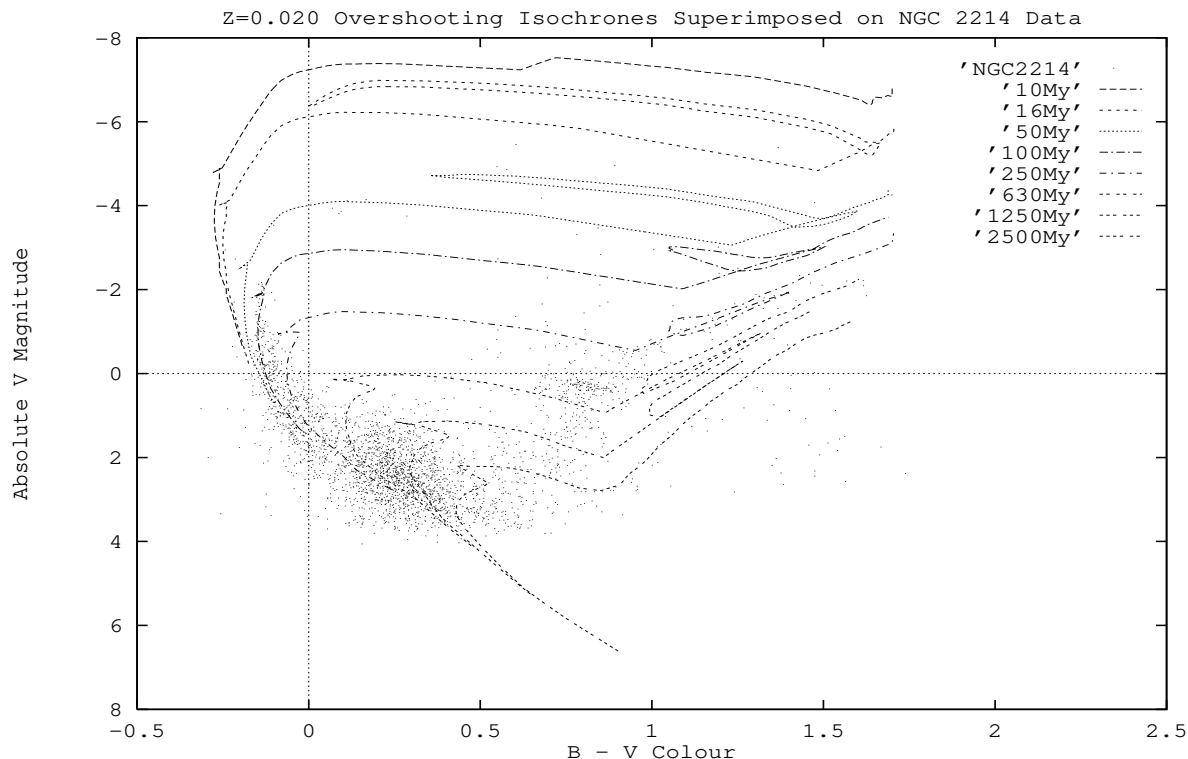


**Figure 9.**  $Z = 0.020$  isochrones superimposed on to the  $BV$  CMD of NGC 2214. Isochrones based on the Schaller et al. (1992) evolution models are plotted over the CMD derived for NGC 2214. The cluster data points have been shifted for a distance modulus of 18.4 mag and reddening of 0.08 mag (see Lee 1992; Castella et al. 1987; Elson 1991). The  $V$  extinction was taken to be 3.1 times  $E(B - V)$ .

Sauvage & Vigroux (1991) give a relation of  $E(B - V)$  increasing by one magnitude for every  $2.4 \times 10^{22}$  atoms per  $\text{cm}^2$  in the LMC. Reddening by this gas would therefore not be detected. Mould, Xystus & Da Costa (1993) give the foreground reddening  $E(B - V)$  for the LMC as 0.07, in agreement with the Galactic reddening maps of Burstein & Heiles (1982), which place NGC 2214 between the 0.06 and 0.09 reddening contours.

The field red giant clump fell on the Swiss 1-Gyr isochrone, although a continuous series of older clumps was present. However, good fits to the lower sections of the subgiant branch required the lower metallicity of 0.004. The  $Z = 0.001$  isochrones were too blue, and could not fit this feature well, whereas the 0.004 isochrones could also fit the slight clumping of stars to the upper left of the giant clump, as well as the few stars above the giant branch (i.e. as being on the asymptotic giant branch). This would be in keeping with the general nature of the age-metallicity relation of Da Costa (1991) for the LMC. The relative densities along the giant clumps also suggest that there was a final burst of field star formation  $\sim 1$ -Gyr ago, after what appears to be continuous formation as evidenced by the extended subgiant branch. Such a conclusion is consistent with the results of Bertelli et al. (1992).

No isochrone could be fitted to the faint red stars given the adopted distance modulus, although their distribution in the CMD resembled a giant branch. The same feature can be seen in the field CMD. If this is a giant branch, then it must belong to a population with a distance modulus greater than that of the cluster. A program was used to

assign an identification number to each star, and could be used to plot the distribution of these stars either on a CMD or on the CCD frame itself, allowing the physical distributions of CMD features to be examined. The faint red stars were not clumped, so another more distant cluster could not have been the cause of the feature. The photometry of these stars was good. None of them exceeded the sharpness and  $\chi$  limits of Bhatia & Piotto (1994), who explained the older supergiant branch of Sagar et al. (1991b) as being due to photometric errors primarily caused by crowding in the central regions of the cluster. For ‘good’ photometry, Bhatia & Piotto (1994) required  $\chi$  to be under 2 and the absolute value of the sharpness to be under 0.5. The faint red stars in the current CMDs had mean sharpness values of  $0.95 \pm 0.13$  and  $1.00 \pm 0.15$ , and mean  $\chi$  values of  $-0.01 \pm 0.05$  and  $0.00 \pm 0.02$ , for the long-exposure  $B$  and  $V$  frames respectively. These objects are therefore entirely consistent with stellar images. It is highly unlikely that they represent images of other objects, such as faint galaxies.

Mateo & Hodge (1986) noted a similar ‘arm’ in the remote LMC cluster NGC 1777, and considered it to be a subgiant branch at least 3-Gyr old, based on Vandenberg’s (1985) isochrones. Bertelli et al. (1992) considered that similar stars in their CMDs were likely foreground objects, according to the counts predicted by Ratnatunga & Bahcall (1985) for the direction of the LMC. A comparison of the cluster CMD given in this study with the predicted star counts given by the Bahcall & Soniera (1980, 1984) galaxy model was made. Observational counts exceeded the predicted ones in all but the region  $V = 21$  to 23 and  $(B - V)$



**Table 3.** Expected field star counts. The predicted star counts of Ratnatunga & Bahcall (1985) for given regions of a CMD for the direction of the LMC are compared with actual star counts from cluster CMDs obtained by this study. The region limits are those given in Ratnatunga & Bahcall (1985). The ‘O’ rows give the observed star counts, while the ‘E’ rows contain the expected numbers.

	$(B - V)$ Colour	V Magnitude Range				
		13-15	15-17	17-19	19-21	21-23
O	0.8-1.3	2	10	132	120	27
E	0.8-1.3	0.7	3.5	7.3	5.9	10
O:	1.3+	3	14	13	19	4
E:	1.3+	0.1	0.8	5.0	17.7	39.5

greater than 1.3 where the observational limit was met (see Table 3). The majority of the enhancements were obviously due to features such as the giant branch. The region  $(V, B - V) = (21-23, 0.8-1.3)$  is to the red of the field main sequence (MS) by more than any of the individual observational errors of MS stars at these magnitudes, and it contains 3 times as many stars as expected from the model, even though the count is not corrected for incompleteness (see below) which will be significant at such faint magnitudes. The photometric errors of these stars do not overlap with those of similarly faint MS stars. The region (19–21, 1.3+) is barely above the expected value, and not statistically significant. However, when counting incompleteness is considered, using the Lesser Completeness Factor Method discussed below, some 26 stars are expected in this region. It appears that foreground contamination or photometric uncertainty (such as these being stars ‘scattered’ off the main sequence) cannot account for all the faint red stars, leaving their origin still unclear.

### 3.5 Aperture photometry

The IRAF IMFORT program of Fischer et al. (1992a) and Fischer, Welch & Mateo (1992b; 1993) was slightly modified to handle the AAT data and used to perform photometry, in a manner similar to Djorgovski (1987), on the 30-s and 60-s  $V$  and  $B$  exposures of both NGC 2214 and the field region. The cluster frames were broken up into a series of concentric elliptical annuli centred on the cluster centre. The same central pixel coordinates were used for the field frames. Each annulus was divided into eight sectors, and the intensity summed within each. The median value was adopted as being representative of the sectors at the weighted average radius, in an attempt to reduce the effect of bright supergiants in the profile (Fischer et al. 1993). The standard error of the sectors is equal to the standard error of the mean multiplied by  $\sqrt{\pi/2}$ , leading to the photometric uncertainty for the annulus.

The program was used with the NGC 1978 Johnson  $B$ -band data of Fischer et al. (1992b), as a check to see that it was performing correctly. In this case an ellipticity of 0.3 was adopted. A smooth luminosity profile was derived, very similar to Fig. 10 of Fischer et al. (1992b), which was reassuring. Tests using a circular aperture showed no significant systematic differences from results using the elliptical aperture, confirming the findings of Fischer et al. (1992b), and

lending support to the contention of Elson et al. (1987) that circular apertures could be used on LMC clusters despite the (small on average) cluster ellipticities.

King (1962) showed that three parameters were needed to describe the structure of globular clusters:

- (i) A core radius ( $r_c$ ), specifying the size of a region of constant density near the cluster centre;
- (ii) A tidal radius ( $r_t$ ), being the tidal limit defined by the gravity of the host galaxy;
- (iii) A scaling factor  $k$ .

The empirical formulation of King (1962) is given as:

$$f = k \left( \frac{1}{\sqrt{1 + \left(\frac{r}{r_c}\right)^2}} - \frac{1}{\sqrt{1 + \left(\frac{r_t}{r_c}\right)^2}} \right)^2$$

where  $f$  is the intensity per pixel (or surface density), and  $r$  the radius. King (1966) comments that his later dynamical models agree closely with the empirical curves. This expression was used as the fitting equation for non-linear least-squares optimizations.

King models were fitted to the  $V$ -band profile of NGC 1978, and the  $V$  and  $B$  profiles of NGC 2214. NGC 1978 was fitted well by the models. A typical result was  $r_c = 12.2 \pm 1.4$ -arcsec and  $r_t = 154 \pm 5$ -arcsec (see Fig. 10). Slightly different starting parameters led to different final values, with ranges of around 10-arcsec  $< r_c < 14$ -arcsec and 140-arcsec  $< r_t < 170$ -arcsec, suggesting that the minimum was rather flat. This was confirmed by a grid search, in which  $r_c$  and  $r_t$  were fixed, leaving only  $k$  to be optimized. A shallow, but fully enclosed, minimum was revealed.

The errors given are based on the photometric errors discussed above, and a Hessian matrix (as in Bevington 1969). This matrix consists of the second-order derivatives of  $\chi^2$  against various parameters and combinations of parameters about the optimum. Mateo, Hodge & Schommer (1986) noted that similar small errors in their  $\chi^2$  minimization King model fits were an illusion, and that many profiles fitted the data nearly as well (see their Fig. 9). However, the derived standard deviations are given below to indicate relative uncertainties between parameters. The core radius value for NGC 1978 agrees well with the 11.2-arcsec estimate of Mateo (1987).

The NGC 2214 data were collected into equal-width log radius bins, with the mean being taken for each populated bin, to avoid implicit weighting of the model fit by more data points being in the outer regions. Fits to both the binned and unbinned values required large values for the tidal radius. Grid searches were also performed on the  $B$  and  $V$  NGC 2214 data. They revealed that, while the core radius was constrained, there was only a lower boundary for the tidal radius. The best  $B$  fit was for radii  $r_c = 9.9 \pm 2.4$ -arcsec and  $r_t = 296 \pm 67$ -arcsec (see Fig. 11). It was repeatedly reached from various starting values, as long as  $r_t$  was initially small. The  $V$ -band result was similar in  $r_c$ , being  $10.6 \pm 2.2$ -arcsec, and the tidal radius was  $258 \pm 190$ -arcsec. The tidal radii were very dependent on the background values adopted – a variation of  $\sim 1$  per cent could cause the radius to vary by nearly a factor of 2. The NGC 2214 radii agree well with the value of  $10.5 \pm 0.7$ -arcsec given by Elson (1991) for the core radius, and the tidal radius range of 125 to 630-arcsec reported by Elson et al. (1987).

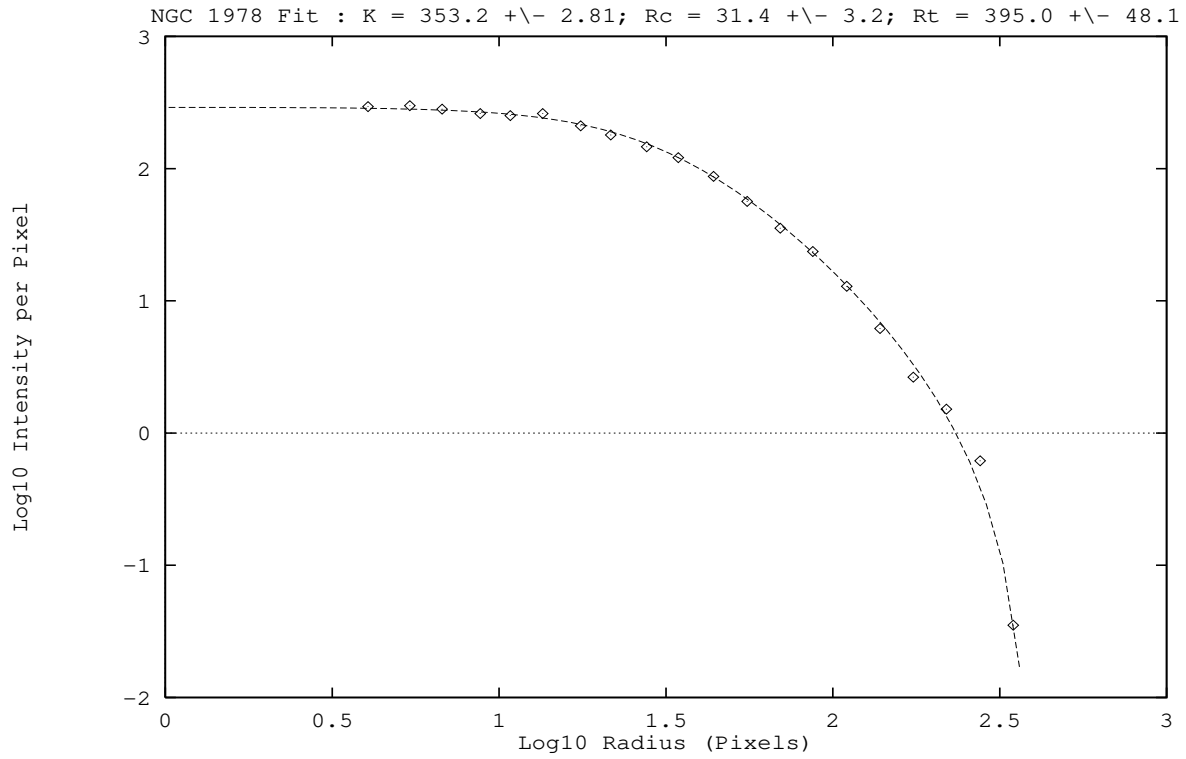


**Figure 10.** King model fit to NGC 1978. The logarithmic binned  $V$  profile for NGC 1978 is shown, with the best-fitting King model.

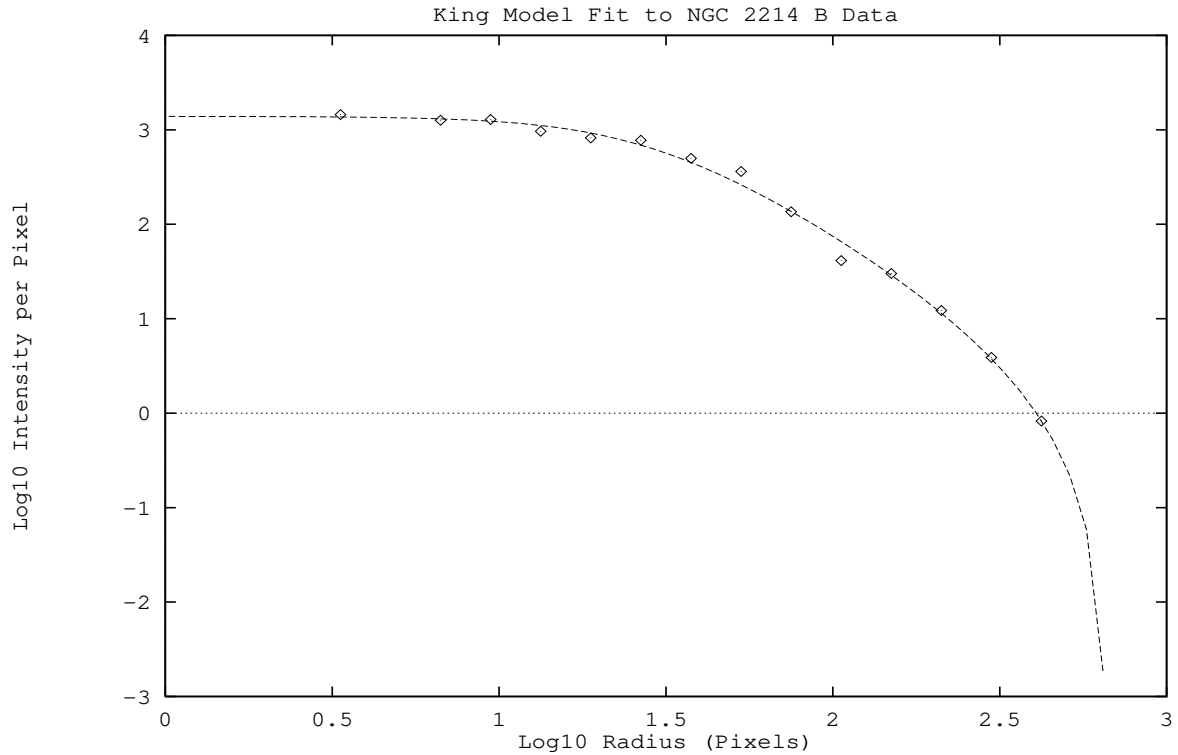


**Figure 11.** King model fit to NGC 2214. The log binned  $B$  profile for NGC 2214 is shown with the best-fitting King model. The gradient for NGC 2214 is shallow and insufficient to provide good constraints on the tidal radius, unlike NGC 1978.

Elson et al. (1987) noted similar problems with constraining the tidal radius in young LMC clusters, and commented that an unbound ‘halo’ of stars about the clusters might be responsible. Given that a King model fits the intermediate-age cluster NGC 1978 well, but not the young cluster NGC 2214, this conclusion is supported by the current study. Elson et al. (1987) introduced a model intended to fit the profiles better:

$$\mu(r) = \mu_0 \left( 1 + \frac{r^2}{a^2} \right)^{-\frac{\gamma}{2}}$$

which gave inconclusive results when it was used as the fitting function to the current NGC 2214 data. The form of this expression was chosen purely for mathematical convenience by Elson et al. (1987). The  $\chi^2$  for the  $B$ -band was  $\sim 75$  per cent better than that of the best King model fit, but the  $V$ -band was  $\sim 44$  per cent worse, making it unclear if the model fitted the data better. The values of the radius  $a$  were  $14.0 \pm 0.2$ -arcsec and  $16.6 \pm 0.2$ -arcsec respectively, which are larger than the value of 11-arcsec (no error given) of Elson et al. (1987). However,  $\gamma$  values of  $2.65 \pm 0.19$  and  $3.05 \pm 0.22$  were obtained for the two profiles. As commented above, the standard deviation errors are an underestimate. The first value of  $\gamma$  is in reasonable agreement with the value of  $2.40 \pm 0.24$  derived by Elson et al. (1987) for the cluster, while the second falls into the range of  $\gamma$  covered by their young cluster sample. Elson (1991) fitted such models to CCD observations of NGC 2214, but did not present the  $\gamma$  values, commenting that they too fell into the same range found by Elson et al. (1987).

There is a potential problem with the aperture photometry program used in this section, in that it simply checks to see if the *centre* of a given pixel falls within an annulus. It does not consider how much of a pixel may fall within the annulus, and scale the intensity appropriately. Such a ragged edge to the annuli may become more important with decreasing radius from the centre, in a region possibly critical for fitting King (1966) models, although these values tend to be within the core radius and so of essentially uniform intensity. This may be countered by the observation above that elliptical and circular apertures resulted in similar profiles. Despite these comments, the program can be used with no reservations to search for colour gradients in the cluster, provided the same parameters are used for the  $B$  and  $V$  frames, and so the same pixels fall into the same apertures. The field showed no colour variation, nor any gradient in star counts. The cluster showed no variation, beyond random scatter, at large radii, and then became increasingly more red with decreasing radius as the ratio of cluster stars to field stars increased. Finally, the colour levelled out within the main body of the cluster, although the cluster is really too small for these results to be definitive. Small-radii colours can be easily affected by individual bright stars.

Aperture photometry was performed on the short-exposure images of the cluster. The aperture radius was 78-arcsec, giving sky-subtracted values of  $V = 10.86$  and  $B - V = 0.36$  mag. This is more red than shallower aperture photometry such as that of van den Bergh & Hagen (1968) and Elson et al. (1987), which only measured the brighter population.

### 3.6 Completeness

The brighter stars in a frame are almost certainly all recovered by the crowded field reduction software. However, certainly not all of the faintest magnitude stars are identified and recovered, with the recovery rate decreasing with increasing magnitude. Problems affecting image recovery include the stars

- (i) simply being so faint that their identification is adversely affected by stochastic variations of the background;
- (ii) being too close to a comparably bright star, leading to a blended elliptical object which will be rejected as not being a star;
- (iii) being lost in the profile of a much brighter star.

A luminosity function that is not ‘corrected’ for these effects will have a more shallow gradient, and with increasing magnitude increasingly underestimate the actual function. Empirical methods of estimating these ‘completeness factors’ generally centre around the addition of artificial stars, or scaled versions of the PSFs derived from selected images, into the CCD frames. These frames are then reduced in an identical manner to the original frame. The efficiency with which these false stars are recovered is taken to estimate the completeness factors, which are then used to correct the observed main-sequence star counts to the values expected if the recovery rate had been 100 per cent. For a given magnitude interval  $i$  the completeness factor is given as:

$$\Lambda_i = \frac{n_{i, \text{recovered}}}{n_{i, \text{added}}} .$$

On a single frame the completeness correction can easily be determined since the variation of the completeness factors with magnitude and crowding can be empirically determined. However, it is not possible to separate main-sequence stars out of the mass of stars. Two colours, such as  $B$  and  $V$ , are required for their identification. The resulting problem of having to match the star image in both colours leads to a further incompleteness. Mateo (1988) and Mateo & Hodge (1986) did not account for this last point, although mention was made of it, and simply considered that the completeness correction for a point  $(V_i, B_i - V_i)$  would be given by:

$$\Lambda(V_i) \times \Lambda(B_i) .$$

Sagar & Richtler (1991) argued that the two frames were not independent and that the multiplicative assumption of Mateo (1988) could not be justified. Instead, as the spatial distribution of stars in the frames is the same and the magnitude distribution is slightly modified, the completeness at a given point in the CMD would be mainly controlled by the lesser of the two completeness factors. There has been no test of the ability of these techniques to recover a known luminosity function.

In order to estimate the completeness factors for our data, an IRAF script was written which placed a small number of artificial stars into a frame. 50 stars was the maximum number of stars added at each iteration by the script (being typically  $\sim 5$  per cent of the detected stars), which meant that the frame crowding and luminosity function would not be greatly affected by the introduction of the artificial stars. A user-selected magnitude range was divided up into bins, typically 0.5 mag wide. ‘Random’ magnitudes and  $(x, y)$  positions were generated for stars in each bin, using the ‘Mini-

**Table 4.** Long exposure completeness factors for the long-exposure *BV* field and cluster frames. Observational magnitudes are used (see text for reasoning). ‘Err’ gives the standard deviation error in the recovery rates.

Range		<i>V</i> field			<i>B</i> field			<i>B</i> cluster				<i>V</i> cluster			
Min	Mag	Out	In	%	Out	In	%	Out	In	%	Err	Out	In	%	Err
14.0	14.5	529	550	96.2	887	900	98.6	3069	3100	99.0	1.8	2435	2450	99.4	2.0
14.5	15.0	531	550	96.5	443	450	98.4	2220	2250	98.7	2.1	2225	2250	98.9	2.1
15.0	15.5	526	550	95.6	442	450	98.2	3485	3550	98.2	1.7	2457	2500	98.3	2.0
15.5	16.0	537	550	97.6	444	450	98.7	1717	1750	98.1	2.4	2168	2200	98.6	2.1
16.0	16.5	535	550	97.3	441	450	98.0	3052	3100	98.4	1.8	3434	3500	98.1	1.7
16.5	17.0	539	550	98.0	448	450	99.6	2591	2650	97.8	1.9	2354	2400	98.1	2.0
17.0	17.5	534	550	97.1	443	450	98.4	3169	3250	97.5	1.5	3573	3650	97.9	1.7
17.5	18.0	535	550	97.3	437	450	97.1	2038	2100	97.0	2.2	3066	3150	97.3	1.8
18.0	18.5	543	550	98.7	442	450	98.2	3801	3950	96.2	1.6	2832	2900	97.7	1.9
18.5	19.0	541	550	98.4	443	450	98.4	2733	2850	95.9	1.9	2649	2750	96.3	1.9
19.0	19.5	537	550	97.6	441	450	98.0	3222	3350	96.2	1.7	3151	3250	96.9	1.7
19.5	20.0	533	550	96.9	433	450	96.2	2489	2650	93.9	1.9	4633	4800	96.5	1.4
20.0	20.5	529	550	96.2	429	450	95.3	2910	3200	90.9	1.8	2268	2450	92.6	2.0
20.5	21.0	514	550	93.5	420	450	93.3	2921	3350	87.2	1.7	1442	1600	90.1	2.5
21.0	21.5	543	600	90.5	409	450	90.9	2921	3500	83.5	1.7	1674	2000	83.7	2.2
21.5	22.0	515	600	85.8	423	500	84.6	1986	2500	79.4	2.0	1633	2100	77.8	2.2
22.0	22.5	538	700	76.9	1060	1350	78.5	3231	4550	71.0	1.5	1781	2450	72.7	2.0
22.5	23.0	727	1200	60.6	422	650	64.9	1990	3200	62.2	1.8	771	1250	61.7	2.8
23.0	23.5	526	1550	33.9	400	850	47.0	1003	2150	46.7	2.2	1627	4000	40.7	1.5
23.5	24.0	236	1500	15.7	291	1050	27.7	536	2250	23.8	2.1	566	2400	23.6	2.0
24.0	24.5	61	550	11.1	60	450	13.3	-	-	-	-	-	-	-	-
Total:		9786	10800	-	9658	12050	-	51084	59520	-	-	47639	54050	-	-

**Table 5.** Short exposure field frames completeness factors are given for the observational magnitudes.

Range		<i>V</i> Field			<i>B</i> Field		
Min	Mag	Out	In	%	Out	In	%
14.0	14.5	711	720	98.8	1155	1170	98.7
14.5	15.0	709	720	98.5	1157	1170	98.9
15.0	15.5	707	720	98.2	1923	1950	98.6
15.5	16.0	705	720	97.9	1932	1950	99.1
16.0	16.5	771	780	98.9	1890	1900	99.5
16.5	17.0	590	600	98.3	1937	1950	99.3
17.0	17.5	769	780	98.6	1223	1230	99.4
17.5	18.0	766	780	98.2	509	510	99.8
18.0	18.5	767	780	98.3	1217	1230	98.9
18.5	19.0	762	780	97.7	768	780	98.5
19.0	19.5	811	840	96.6	1146	1170	97.9
19.5	20.0	799	840	95.1	1184	1230	96.3
20.0	20.5	2294	2400	95.6	1180	1230	95.9
20.5	21.0	1446	1560	92.7	414	450	92.0
21.0	21.5	732	840	87.1	1148	1450	79.2
21.5	22.0	1431	1860	76.9	1112	2790	39.9
22.0	22.5	1416	2700	52.4	107	1050	10.2
22.5	23.0	322	1800	17.9	-	-	-
Total:		16448	20220	-	20002	23210	-

mal Standard’ pseudo-random number generator of Park & Miller (1978). Press et al. (1992, p. 279) note that the period of this generator is  $2^{31} - 1$ .

Several sets of false stars were added to the frame (in different iterations) and reduced until a user-set limit of recovered false stars was met. This limit was set high since the completeness factors vary with crowding. In a frame of a LMC star cluster, the degree of crowding naturally varies across the frame. Mateo (1988) divided frames into three rings centred on the cluster, surrounded by field, and formed a mean luminosity function from these rings. Rather than

adopt this technique, and its assumptions (see Mateo 1988), we chose to derive a mean by placing many stars into the frames.

Several IRAF scripts were written to test techniques for estimating completeness factors. The tests involved the creation of artificial field frames with known luminosity functions. The completeness techniques were then used to estimate these functions. These estimates could be compared with the actual function. Details of these tests can be found in Banks (1994). The product method of Mateo (1988) was found increasingly to overestimate the completeness correction as magnitude increased. The Lesser Ratio method recovered the actual luminosity function better, with a mean error of  $\sim 3$  per cent, although near the observational limit of the frames the technique underestimated the function. The technique assumed that all the false stars recovered on the frame producing the lower completeness factor were all recovered on the second frame. Towards fainter magnitudes, recovery rates drop and so this assumption cannot hold. Another computer program was written to test the effect of this assumption. Stars *with* colour were placed into both the *B* and *V* frames, and recovered in the same manner as the ‘real stars’ were. This dual-frame method estimated the recovery rates better than the other techniques, except when the factor fell below 50 per cent, which Stetson (1991) defines as the limiting magnitude of a CCD frame. However, the technique is *extremely* computer-intensive, making use of it prohibitive if it is to be used over the entire magnitude range of the frames. Fortunately, the matching problem will only affect completeness estimates near the faint limit of the images, allowing the simpler Lesser Ratio method to be used for the bulk of the calculations.

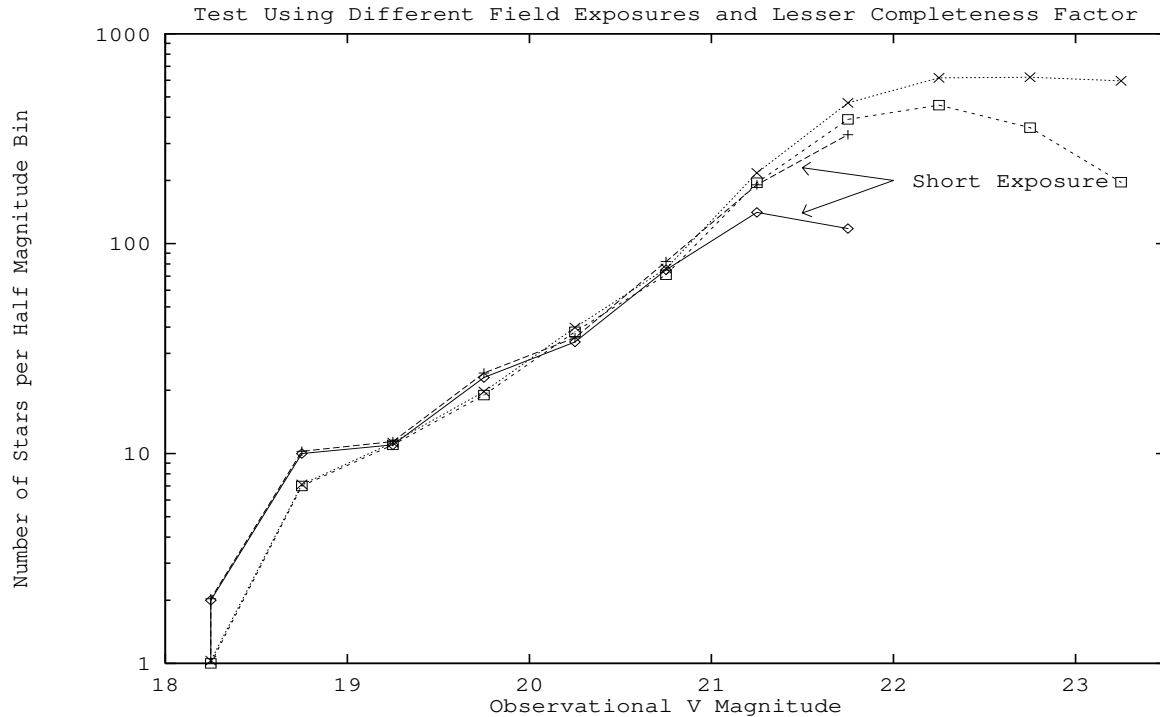


**Figure 12.** Observational  $V$ -band luminosity functions. The long- and short-exposure  $V$ -band luminosity functions, with no attempt to remove non-main-sequence stars, are plotted both with and without the appropriate completeness corrections applied. The uncorrected (raw) data are given by  $\diamond$  and  $\square$  for the short and long exposures respectively, while the corrected values are indicated by  $+$  and  $\times$  symbols.

The results of the completeness factor trials on the long-exposure frames are given in Table 4. More artificial stars were added to the cluster frames in an attempt to account for the variation in crowding across the frames.

The completeness factors for the short-exposure field frames are in Table 5. These values were used in conjunction with the Lesser Ratio method to ‘correct’ the short-exposure  $V$  luminosity function. Similarly, values from Table 4 were used to correct the long-exposure  $V$  function. This was to test whether the same ‘real’ function would be recovered from the two exposures. It was found to be true in general, except for the brightest and faintest magnitudes (see Fig. 12). The difference at faint magnitudes is likely to be due to the matching problem mentioned above (which led to the dual-frame method), which will become more apparent near the limiting magnitude. Use of the dual-frame completeness script seems to be warranted when the individual frame completeness factors fall below  $\sim 75$  per cent. The flattening of the long-exposure  $V$  luminosity function shown in Fig. 12 lies in such a range.

The difference at bright magnitudes is due to saturation of stars in the longer exposures. The position of a star within the cluster will affect its recovery, depending on the star’s magnitude. Bright stars, no matter where they are in a frame, will be saturated in a suitably long exposure. However, there will be a magnitude range where location does matter. If such a star is in a relatively uncrowded region of the frame, it will not be saturated. However, if it is in a crowded region then its light, combined with the fainter

stars that it is covering, will cause the stellar image to saturate.

### 3.7 Field star subtraction

Field stars need to be statistically subtracted from the luminosity function of the cluster. Cluster membership itself is hard to assess in the LMC. Even if radial velocities are available for all the stars, Freeman, Illingworth & Oemler (1983) showed young clusters to have disc dynamics, making such data rather uninformative about membership, only excluding Galactic stars. Flower et al. (1980) and Olszewski (1984) subtracted a star from the cluster CMD for every star within the same given region in the field CMD. This technique ignored completeness factors being different between the field and the cluster. Mateo & Hodge (1986) adjusted the number of stars in both the field and the cluster by their completeness factors and also by the ratio of the areas of the field and cluster regions.

A computer program was written to subtract field stars from the cluster frame listing. Both the  $B$  and  $V$  lists were based on the long-exposure frames. The observational CMD could be divided up into a  $(B, V)$  or a  $(V, B - V)$  grid, or into circular regions about each star in the cluster frame. Regardless of which of the three methods was used to bound a region in the CMD, the numbers of stars within this region in the field and cluster CMDs were counted. The completeness factors for the region centre in both the field and cluster CMDs were used to adjust the star counts. The se-

lected regions therefore should not be too large, otherwise the completeness factors would vary within the region itself. The completeness corrected cluster to field ratio was taken as the probability that a given star (within the region) in the cluster star list was actually a cluster member. If a grid was being used then a random number was generated for each cluster list member within the region. If the random number fell above the probability given by the corrected ratio, the star was considered to be a cluster member, otherwise it was removed from the list. In the case of the circular regions, the probability was applied only to the central star, as all the stars in the cluster frame would be checked in turn. It should be noted that the cluster star list was not altered during the execution of the program. Artificial star and completeness factor lists were used to test the software, which performed as expected. Given the result of the completeness tests, the lesser of the appropriate  $B$  and  $V$  completeness factors was used in the analysis of NGC 2214.

### 3.8 Luminosity functions

The field-star-subtracted star lists need to be corrected for counting incompleteness, before a luminosity function can be estimated. The field star subtraction discussed above only compared the cluster and field ratios in order to calculate a probability that a given star in the cluster CMD was a field member. Mateo (1988) commented that the calibration of the false star magnitudes was problematic as transformation equations explicitly involve a colour term, and so assumed that all his false stars had a  $(B - V)$  colour of 0.5 mag.

To overcome this problem a bin distribution was selected for the  $V$  and  $B$  luminosity functions. The standardized magnitudes of each star were in turn transferred back to the observational system using the transformation equations given above. The relevant  $B$  and  $V$  completeness factors were then referenced, and the appropriate completeness ratio (Mateo, Lesser, or Greater) chosen. The standardized magnitudes were used to determine which luminosity function bins should be altered. The appropriate bin counts were then incremented by the inverse of the completeness ratio. This technique avoided the problem of standardizing the false star magnitudes. The program output results at every step of the process during testing. These values were compared with manual calculations, and found to be correct.

In addition, only main-sequence stars should be included in a luminosity function. Following Mateo (1988), a line was arbitrarily drawn between main-sequence and evolved stars, with the evolved stars being discarded. The importance of using two-colour photometry to define main-sequence stars belonging to a cluster can be illustrated by the Da Costa (1982) luminosity function for the Galactic globular cluster 47 Tuc. A series of single-colour plates was used, producing a relatively steep luminosity function. Later  $BV$  CCD photometry of the cluster by Harris & Hesser (1985) revealed that there was severe contamination of the cluster photometry by faint SMC stars. Removal of these stars flattened the luminosity function to the point where 47 Tuc appears to have one of the flattest luminosity functions amongst the globular clusters.

Several ‘subtractions’ were performed with different seeds for the pseudo-random number generator, producing similar results. The individual search option was used, with

a search radius of 0.282-mag. This corresponds to the same area as that of a 0.5 square magnitude box, or roughly 1.4 times the area of a given combined completeness bin. The intention was to use a search area large enough to collect a reasonable number of stars to avoid low-number statistics, yet not so large that the completeness corrections varied substantially with the region. Given that completeness factors were calculated for 0.5-mag bins in each frame, it was an arbitrary decision to use a region slightly larger than a completeness ‘diamond’ (see Fig. 10 in Mateo 1988) in order to satisfy these two requirements.

### 3.9 Mass functions

The luminosity functions were converted into mass functions using the best fitting Swiss isochrone discussed above ( $Z = 0.020$  with a logarithm age of 8.0) to derive a mass–luminosity function for the cluster. The evolution in luminosity of a star still on the main-sequence can be quite substantial. The change in luminosity between the zero age main-sequence and the turnoff of a star can correspond to between 0.5 and 1.6 mag, depending on the mass of a star (Mateo 1988). We note that the global mass function slope does not sensitively depend on the evolutionary models used (see Mateo (1988) and Sagar & Richtler (1991) who compare mass functions derived using classical and overshooting stellar models). As Mateo (1993) points out, the mass range being studied changes, but the gradient remains effectively the same with the greatest variation occurring below  $Z = 0.004$ .

The resulting mass functions derived from the long-exposure frames are given in Fig. 13. Functions were calculated from both the  $B$  and  $V$  luminosity functions, and are displayed. The errors shown are the Poisson errors in the number of actually retrieved stars (i.e. before the star numbers were corrected for completeness) combined with uncertainty in the completeness correction. The error in the completeness factors themselves is hard to quantify. Poisson errors were assumed for them (as in Table 4). Their inclusion could be quite involved – as the stars falling into a given bin could belong to subgroups each with a different completeness correction. In order to have an upper estimate, the largest of the completeness correction errors was used for the entire group. Linear least-squares fitting was performed on the functions. Using the expression for the IMF introduced in Section 1,  $x$  values of  $1.18 \pm 0.18$ ,  $1.47 \pm 0.21$ , and  $1.32 \pm 0.14$  were derived for the  $B$ ,  $V$ , and combined  $BV$  data. These gradients are in reasonable agreement with Sagar & Richtler (1991), who calculated  $x$  values of  $1.1 \pm 0.3$ ,  $2.2 \pm 0.3$ ,  $1.4 \pm 0.5$ , and  $1.3 \pm 0.3$  for NGC 2214, using the lesser of the  $BV$  completeness factors and different stellar evolution models.

Like the results of Sagar & Richtler (1991), the mass function for NGC 2214 appears to have a steep gradient at the higher masses. They made no comment about this feature, and applied a single straight line. The steep decline in the two most massive  $V$  bins, and the most massive  $B$  bin, is an artefact of the reduction process. While an isolated star with a magnitude that fell into one of these bins would not be saturated on the real frame, it would be if the star were in a region with an enhanced background level, e.g. the cluster centre. Unfortunately, no clipping level corresponding to that used in the reduction of actual observations was set for

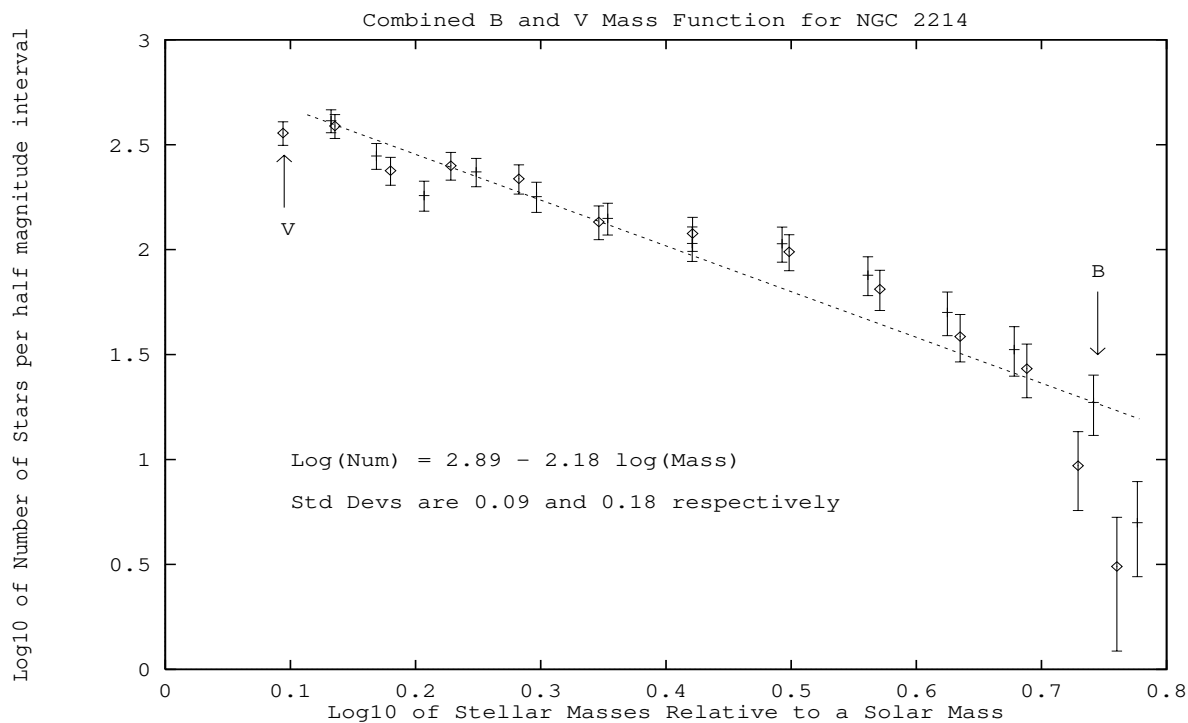


**Figure 13.** Mass function for NGC 2214 based on the long-exposure frames. Values calculated from *B* magnitudes are given as horizontal dashes, while the *V*-based ones are marked by diamonds. The dashed line is the linear least-squares fit to the *B*-data, and its parameter values are given.

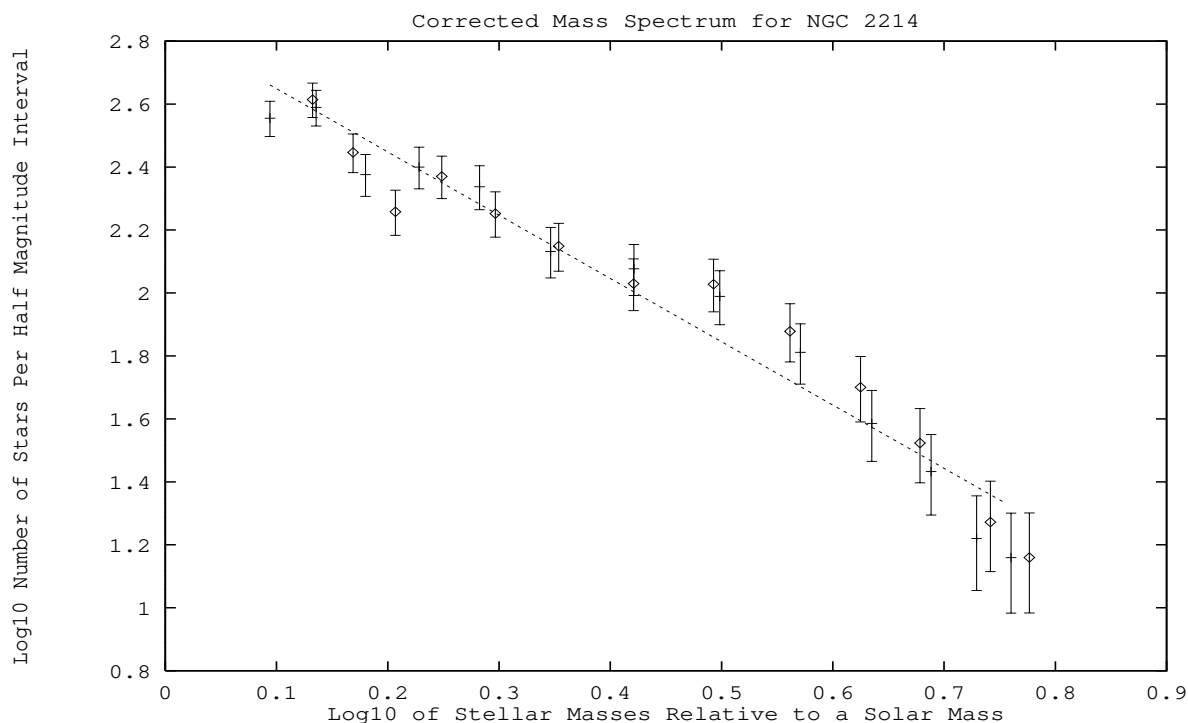


**Figure 14.** Mass function for NGC 2214. The same symbols are used as in Fig. 13, but the high-mass bins are based on the short-exposure frames. The line of best fit given in the previous figure is shown, to ease comparison between the diagrams, and to demonstrate just how uncertain the gradient is.

the artificial star trials. The artificial stars were therefore not rejected even if they were in the cluster centre, leading to an overestimate of the completeness factor on these, the brightest of the bins. It is possible that the same effect was present in the artificial star trials of Sagar & Richtler (1991).

The short-exposure frames were examined for the number of stars that fell into these bins. The numbers were substantially larger, and brought the mass spectrum values of the bins up (see Fig. 14). There is still some hint that two lines could be fitted to the high- and low-mass stars. An  $x$  value of 2 fits the  $\geq 3M_{\odot}$  stars well. Below  $\sim 3M_{\odot}$  a shallower gradient appears reasonable, corresponding to an  $x$  value of 0.8. The combined cluster mass function of Mateo (1988) was over effectively the same range as that of this study. He suggested that the low-mass end ( $\log M/M_{\odot} < 0.45$ ) was slightly steeper. We have found that the incompleteness technique of Mateo (1988) under-estimates recovery rates, with the discrepancy increasing as the completeness rates decline. Therefore our gradients are substantially less than those of Mateo (see Sagar & Richtler (1991) who applied the same completeness technique corrections to NGC 1711, which was the only cluster in common with Mateo (1988), and derived a similar gradient to that found in the present study). The steep gradients of Mateo are not confirmed; nor are the very shallow gradients of Elson et al. (1989).

We considered the possibility that the change in gradient was due to incorrect estimation of the recovery rates at faint magnitudes. The dual-frame completeness script was therefore used on the cluster and field frames. The bins were 0.5 mag wide over the observational  $V$  magnitude range 20–23, and were centred on the main-sequence with a  $(B - V)$  width of 0.30. These bins were selected as per the discussion at the end of Section 3.8. In the case of the current data, no advantage was gained. The estimated completeness factors were within  $1.2 \pm 0.7$  per cent of those estimated by the lesser completeness factor method. This result raises the question of whether more complicated dual-frame completeness techniques, employing a variant of the matrix method proposed by Drukier et al. (1988) to measure the effect of the bin migration discussed above, would be worthwhile in practice.

Linear least-squares fits to the  $B$ ,  $V$ , and combined  $B$  and  $V$  mass spectra (of all the data points) resulted in  $x$  values of  $0.96 \pm 0.14$ ,  $1.06 \pm 0.13$ , and  $1.01 \pm 0.09$  respectively. While this is shallower than the Sagar & Richtler (1991) values for NGC 2214, we note that we can recover similar values before we correct the saturation problem discussed above, and that the new values are in reasonable agreement with the average value of  $x = 1.1$  of Sagar & Richtler (1991) for their five LMC clusters overall for the mass range 1.9–6.3  $M_{\odot}$ .

Sagar & Richtler (1991) investigated the effect that binary stars have on mass functions, finding that the slope of the actual mass function determined the effect itself. Steep mass functions are weighted towards low-mass stars. Therefore since the secondary component of a binary is likely to be less massive than the primary, and so causing little change in the luminosity of the system. Alternatively, flat distributions will produce binaries with mass ratios closer to unity, dramatically affecting the system luminosity (Mateo 1993). Sagar & Richtler (1991) found that mass functions with gra-

dients of 2.5 or steeper were essentially unaffected by binaries, while a mass function of slope 1.5 could be lowered by 0.4 in the extreme case of every star being binary. While the actual proportion of binary stars in LMC clusters is unknown, the work of Sagar & Richtler (1991) indicates that the gradients derived by studies similar to this one are underestimates of the actual gradient.

Mateo (1993) and Banks (1994) review results of mass function studies of Magellanic Cloud clusters. They note that these estimates are all similar, despite being for quite different mass ranges and metallicities – suggesting the possibility of a global IMF in the Clouds. There is poor agreement between mass function estimate studies of the solar neighbourhood (see Banks 1994), emphasizing the difficult nature of this work (see Scalo 1986 for a full discussion of the problems and assumptions involved). It is unclear whether the IMF of young Magellanic Clusters (MC) and Associations is different from Galactic values, and no definite conclusions can be made on the universality of the IMF, based on these results, at present. It has been suggested that the IMF will flatten with decreasing metallicity (see e.g. Terlevich & Melnick 1985; Piotto 1991), and it could be argued that the MC IMFs are flatter – although it should be noted that isochrones of solar neighbourhood metallicity provided the best fit to the NGC 2214 CMD, and there does not appear to be any difference between Galactic halo and disc field star IMFs over the small mass range of 0.3 to 0.8  $M_{\odot}$  (Scalo 1986). Further study is required, including the estimation of the mass functions of LMC clusters with substantially different metallicities.

## 4 CONCLUSIONS

We have found no evidence supporting the contention that NGC 2214 is a merging cluster. Models have been fitted to radial profiles of the cluster, and support the contention of Elson et al. (1987) that an unbound halo of stars causes poor fits by King models. Techniques for evaluating completeness methods have been tested, with the method of Mateo (1988) being shown to underestimate completeness factors. The best techniques were employed on the AAT data, leading to an estimate of the cluster’s mass function, with an  $x$  value of  $\sim 1$ , which is in good agreement with other studies of young Magellanic Cloud clusters. IMF estimates for Galactic regions are unreliable, which makes any conclusions about the universality of the IMF indistinct. However, there are no *substantial* differences between IMFs derived for the Magellanic Clouds and for our Galaxy, and it is likely that star formation in these three galaxies can be described by a ‘universal’ IMF, at least over the mass interval  $\sim 1$  to  $\sim 10 M_{\odot}$ .

## ACKNOWLEDGMENTS

The authors are grateful to Dr G. Da Costa and the AAO for service observing by the Anglo-Australian Telescope, Acorn NZ for the loan of an R260, Dr D. Schaerer for isochrone tables, Dr Phillippe Fischer for his aperture photometry program, Dr J. Scalo for offprints, the Institute of Statistics and Operations Research (Victoria University of Wellington) for



extra computing facilities, Dr M. Mateo for his helpful comments as Referee for this paper, and the Foundation for Research, Science and Technology of New Zealand for partial funding of this project in conjunction with the VUW Internal Research Grant Committee. TB acknowledges partial support during this study by the inaugural Royal Society of New Zealand R.H.T. Bates Postgraduate Scholarship. IRAF is courtesy of the National Optical Astronomical Observatories, which are operated by the Association of Universities for Research in Astronomy, Inc., under cooperative agreement with the US National Science Foundation. The Space Telescope Science Data Analysis System (STSDAS) is courtesy of the Space Telescope Science Institute, Baltimore.

## REFERENCES

- Bahcall J.N., Soniera R.M., 1980, *ApJS*, 44, 73  
 Bahcall J.N., Soniera R.M., 1984, *ApJS*, 55, 67  
 Banks T., 1993, *South. Stars*, 35, 33  
 Banks T., 1994, PhD Thesis, Victoria University of Wellington, New Zealand  
 Banks T., Dodd R.J., Sullivan D.J., 1994, submitted to *Southern Stars*.  
 Banks T., Dodd R.J., Sullivan D.J., 1995, accepted by *MNRAS*  
 Becker S.A., 1981, *ApJS*, 45, 475  
 Bertelli G., Betto R., Bressnan A., Chiosi C., Nasi E., Vallenari A., 1990, *A&AS*, 34, 229  
 Bertelli G., Mateo M., Chiosi C., Bressnan A., 1992, *AJ*, 388, 400  
 Bevington P.R., 1969, *Data Reduction and Error Analysis in the Physical Sciences*. McGraw-Hill, New York  
 Bhatia R.K., MacGillivray H.T., 1988, *A&A*, 203, L5  
 Bhatia R., Piotto G., 1993, in Smith G.H., Brodie J.P., eds, *PASP Conf. Ser. 48, The Globular Cluster–Galaxy Connection*. p. 400  
 Bhatia R., Piotto G., 1994, *A&A*, 283, 424  
 Brunish W.M., Truran J.W., 1982, *ApJS*, 49, 447  
 Burstein D., Heiles C., 1982, *AJ*, 87, 1165  
 Castella A., Barbero J., Geyer E.H., 1987, *ApJS*, 64, 83  
 Castellani V., Chieffi A., Straniero O., 1990, *ApJS*, 64, 83  
 Cayrel R., Tarrab I., Richtler T., 1988, *ESO Messenger*, 54, 29  
 Chiosi C., 1989, *Rev. Mex. Astron. Astrofis.*, 18, 125  
 Da Costa G., 1982, *AJ*, 87, 990  
 Da Costa G., 1991, in Haynes R., D. Milne D., eds, *Proc. IAU Symp. 148, The Magellanic Clouds*. Kluwer, Dordrecht, p. 183  
 Djorgovski S., 1987, in Grindlay J., Philip A.G.D., eds, *Proc. IAU Symp. 126, Globular Cluster Systems in Galaxies*. Reidel, Dordrecht, p. 333  
 Drukier G.A., Fahlman G.G., Richer H.B., Vandenberg D.A., 1988, *AJ*, 95, 1415  
 Elson R.A.W., 1991, *ApJS*, 185, 76  
 Elson R.A.W., Fall S.M., Freeman K.C., 1987, *AJ*, 323, 54  
 Elson R.A.W., Fall S.M., Freeman K.C., 1989, 336, 734  
 Fischer P., Welch D.L., Côté P., Mateo M., Madore B.F., 1992a, *AJ*, 103, 857  
 Fischer P., Welch D.L., Mateo M., 1992b, *AJ*, 104, 1086  
 Fischer P., Welch D.L., Mateo M., 1993, *AJ*, 105, 938  
 Flower P., Geisler D., Hodge P., Olszewski E., 1980, *ApJ*, 235, 769  
 Freeman K.C., Illingworth G.D., Oemler A., 1983, *ApJ*, 272, 488  
 Frenk C.S., Fall S.M., 1982, *MNRAS*, 199, 565  
 Graham J., 1982, *PASP*, 94, 244  
 Harris W.E., Hesser J.E., 1985, in Goodman J., Hut P., eds, *Proc. IAU Symp. 113, The Dynamics of Star Clusters*. Dordrecht, Reidel, p. 81  
 Jasniewicz G., Thévenin F., 1994, *A&A*, 282, 717  
 Jedrzejewski R.I., 1987, *MNRAS*, 226, 747  
 King I.R., 1962, *AJ*, 67, 471  
 King I.R., 1966, *AJ*, 71, 64  
 Lee M.G., 1992, *ApJ*, 399, L133  
 MacGillivray H.T., Stobie R.S., 1984, *Vistas Astron.*, 27, 433  
 Maeder A., Meynet G., 1991, *A&AS*, 89, 451  
 Mateo M., 1987, *ApJ*, 323, L41  
 Mateo M., 1988, *ApJ*, 331, 261  
 Mateo M., 1993, in Smith G.H., Brodie J.P., eds, *PASP Conf. Ser. 48, The Globular Cluster–Galaxy Connection*. p. 387  
 Mateo M., Hodge P., 1986, *ApJS*, 60, 893  
 Mateo M., Hodge P., Schommer R.A., 1986, *ApJ*, 311, 113  
 Mathewson D., Ford V., 1983, in van den Bergh S., de Boer K., eds, *Proc IAU Symp. 108 Structure and Evolution of the Magellanic Clouds*. Reidel, Dordrecht, p. 127  
 Meylan G., Djorgovski S., 1987, *ApJ*, 322, L91  
 Meynet G., Mermilliod J.-C., Maeder A., 1993, *A&A*, 98, 447  
 Mould J.R., Xystus D.A., Da Costa G.S., 1993, *ApJ*, 408, 108  
 Olszewski E., 1984, *ApJ*, 284, 108  
 Park S.K., Miller K.W., 1978, *Comms. ACM*, 31, 1192  
 Phelps R.L., Janes K.A., 1993, *AJ*, 106, 1870  
 Piotto G., 1991, in Janes K., ed, *ASP Conf. Ser. 13, The Formation and Evolution of Star Clusters*. p. 200  
 Press W.H., Teukolsky S.A., Vetterling W.T., Flannery B.P., 1992, *Numerical Recipes in C: The Art of Scientific Programming*, Second Edition. Cambridge University Press  
 Ratnatunga K.U., Bahcall J.N., 1985, *ApJS*, 59, 63  
 Reid N., 1992, *MNRAS*, 257, 257  
 Richtler T., Nelles B., 1983, *A&A*, 119, 75  
 Richtler T., Spite M., Spite F., 1989, *A&A*, 225, 351  
 Rieke G.H., Lebofsky M.J., 1985, *AJ*, 288, 615  
 Robertson J.W., 1974, *A&AS*, 15, 261  
 Sagar R., Richtler T., 1991, *A&A*, 250, 324  
 Sagar R., Richtler T., de Boer K.S., 1991a, *A&A*, 249, L5  
 Sagar R., Richtler T., de Boer K.S., 1991b, *A&AS*, 90, 387  
 Salpeter E.E., 1955, *ApJ*, 121, 161  
 Sauvage M., Vignoux L., 1991, in Haynes R., Milne D., eds, *Proc. IAU Symp. 148, The Magellanic Clouds*. Kluwer, Dordrecht, p. 407  
 Scalo J.M., 1986, *Fundam. Cosmic Phys.*, 11, 1  
 Schaerer D., Meynet M., Maeder A., Schaller G., 1993, *A&A*, 98, 523  
 Schaller G., Schaerer D., Meynet G., Maeder A., 1992, *A&A*, 96, 269  
 Spite M., Cayrel R., Francois P., Richtler T., Spite F., 1986, *A&A*, 168, 197  
 Spitzer L., Jr., 1987, *Dynamical Evolution of Globular Clusters*, Princeton Series in Astrophysics. Princeton University Press, New Jersey, USA  
 Stauffer J., Klemola A., Prosser C., Probst R., 1991, *AJ*, 101, 980  
 Stetson P.B., 1987, *PASP*, 99, 191  
 Stetson P.B., 1991, in Janes K., ed, *ASP Conf. Ser. 13, The Formation and Evolution of Star Clusters*. p. 88  
 Terlevich R., Melnick J., 1985, *MNRAS*, 213, 841  
 Tinsley B.M., 1980, *Fundam. Cosmic Phys.*, 5, 287  
 van den Bergh S., Hagen G.L., 1968, *AJ*, 73, 569  
 Vandenberg D.A., 1985, *ApJS*, 558, 711  
 Zepka A.F., Dottori H.A., 1987, *Rev. Mex. Astron. Astrofis.*, 14, 172

This paper has been produced using the Royal Astronomical Society/Blackwell Science  $\LaTeX$  style file.